


Article

# Nucleation of $\{10\bar{1}2\}$ Twins in Magnesium through Reversible Martensitic Phase Transformation

Jamie Ombogo <sup>†</sup>, Amir Hassan Zahiri <sup>†</sup> , Tengfei Ma  and Lei Cao <sup>\*</sup> 

Mechanical Engineering Department, University of Nevada, Reno, NV 89557, USA; mr.tm@nevada.unr.edu (J.O.); azahiri@nevada.unr.edu (A.H.Z.); tengfeim@nevada.unr.edu (T.M.)

<sup>\*</sup> Correspondence: leicao@unr.edu

<sup>†</sup> These authors contributed equally to this work.

Received: 27 June 2020; Accepted: 26 July 2020; Published: 1 August 2020



**Abstract:** We report the discovery of a rigorous nucleation mechanism for  $\{10\bar{1}2\}$  twins in hexagonal close-packed (hcp) magnesium through reversible hcp-tetragonal-hcp martensitic phase transformations with a metastable tetragonal phase as the intermediate state. Specifically, the parent hcp phase first transforms to a metastable tetragonal phase, which subsequently transforms to a twinned hcp phase. The evanescent nature of the tetragonal phase severely hinders its direct observation, while our carefully designed molecular dynamics simulations rigorously reveal the critical role of this metastable phase in the nucleation of  $\{10\bar{1}2\}$  twins in magnesium. Moreover, we prove that the reversible hcp-tetragonal-hcp phase transformations involved in the twinning process follow strict orientation relations between the parent hcp, intermediate tetragonal, and twin hcp phases. This phase transformation-mediated twinning mechanism is naturally compatible with the ultrafast twin growth speed. This work will be important for a better understanding of the twinning mechanism and thus the development of novel strategies for enhancing the ductility of magnesium alloys.

**Keywords:** twinning; magnesium; martensitic phase transformation; molecular dynamics

## 1. Introduction

The application of hexagonal close-packed (hcp) magnesium (Mg) alloys as lightweight structural components in automotive and aerospace industries has been severely limited by their inferior ductility [1,2], which necessitates a rigorous understanding of the deformation mechanisms of Mg. It is now well understood that the brittleness of Mg arises from its largely anisotropic critical resolved shear stress between basal slip and non-basal slip, and thus restricted number of easily activated slip systems. Accordingly, extensive efforts have been devoted to exploring the activation of deformation twinning in Mg [1,3–12], which is an important category of deformation mode to meet the von Mises' criterion that there must be at least five independent deformation modes for a crystal to undergo an arbitrarily imposed deformation. However, the nucleation mechanism of the  $\{10\bar{1}2\}$  twin [9,10,13–22], which is the predominant twinning mode in Mg, still remains elusive. The earliest nucleation model describes the homogeneous nucleation of twins due to high stress concentration [5,16,17,23]. However, the chance of the occurrence for this process was believed to be extremely low due to the required extremely high stress. Subsequent studies have focused on heterogeneous nucleation through the gliding of disconnections generated by the dissociation of pre-existing defects, such as various types of dislocations [18–20,24], dislocation pile-ups [14], grain boundary defects [13], and prismatic/basal interfaces [22,25].

In this work, we report the discovery of the nucleation of  $\{10\bar{1}2\}$  twins in Mg through reversible martensitic phase transformations, which is naturally compatible with the ultrafast twin growth speed. We emphasize the significance of an evanescent tetragonal phase, which serves as a critical

intermediate state that seamlessly bridges the crystallographic planes of the parent hcp phase and twinned hcp phase throughout the phase transformation-mediated twinning process. This work, rigorizing the existing twinning mechanism of the  $\{10\bar{1}2\}$  twin in Mg and unveiling the essential role of the metastable tetragonal phase, will pave the way for the rational development of physics-guided strategies for enhancing the ductility of Mg alloys.

The rest of this paper is organized as follows. Section 2 describes the methodology of this work. In Section 3, we present our findings of the martensitic phase transformation-mediated  $\{10\bar{1}2\}$  twinning process. We also analyze the detailed structure of the metastable tetragonal phase and the orientation relation during the reversible martensitic phase transformation. In addition, the atomic motion in our mechanism is compared with that in the twinning dislocation-based mechanism. Finally, we conclude this paper in Section 4.

## 2. Methodology

In this work, molecular dynamics (MD) simulations are performed using the Large-scale Atomic/Molecular Massively Parallel Simulator (LAMMPS) package [26] with a time-step size of 1 fs. The interactions between Mg atoms are modeled by an embedded-atom method potential developed by Wilson et al. [27]. The simulation domain with a size of  $32 \times 27 \times 26 \text{ nm}^3$  contains one million hcp atoms and periodic boundary conditions are applied in all directions. We first use MD to perform melt-quenching of the simulation domain, which generates a nanotwinned Mg with a twin spacing of  $\sim 10 \text{ nm}$ . This nanotwinned structure contains parallel  $\{10\bar{1}1\}$  twins, long partial stacking faults, and dislocations, as shown in Figure 1a. Then, we apply a compressive strain (up to 20%) along the  $x$ -direction, which is approximately parallel to the initial  $\{10\bar{1}1\}$  twin boundaries, with a strain rate of  $10^8 \text{ s}^{-1}$  and a temperature of 10 K. The reason for choosing this particular direction of deformation is to demobilize the  $\{10\bar{1}1\}$  twins to avoid their interference with the nucleation process of the  $\{10\bar{1}2\}$  twins studied in this work. Finally, we use the Open Visualization Tool (OVITO) [28] to visualize and analyze the microstructure evolution during the deformation process. The crystalline structures are identified using the common neighbor analysis [29,30], with hcp, body-centered cubic-like (tetragonal), face-centered cubic (fcc), and amorphous phases denoted by the color of cyan, red, green, and yellow, respectively.

## 3. Results and Discussion

### 3.1. The Formation of $\{10\bar{1}2\}$ Twins

In this section, we will demonstrate the deformation process of the Mg structure and the formation of  $\{10\bar{1}2\}$  deformation twins. Figure 1 shows the microstructure evolution in our MD simulation up to an applied strain of 5.52%. When the applied strain reaches 3.24%, we observe a sudden hcp-to-tetragonal martensitic phase transformation. The metastable tetragonal phase is indicated by the arrow in Figure 1b and its atomic structure will be demonstrated in details in the next section. Then, the tetragonal phase grows quickly and reaches its maximum size at a strain of 3.92%, as shown in Figure 1c. Finally, as shown in Figure 1d, the reverse tetragonal-to-hcp martensitic phase transformation converts the tetragonal phase back into an hcp phase that is misoriented from the parent hcp phase, resulting in two twin boundaries in between. As shown by the close-up view in Figure 1g, the misorientation between the basal planes of the parent hcp phase and the newly formed hcp phase is  $\sim 87^\circ$  across a common  $a$ -axis, which matches the theoretical value of the  $\{10\bar{1}2\}$  extension twin.

After the nucleation process, one of the  $\{10\bar{1}2\}$  twin boundaries propagates quickly across the simulation domain, as indicated by the arrows in Figure 1d,e. The fast migration of the twin boundary leaves behind many partial stacking faults, that is, a single layer of fcc atoms. Finally, this mobile twin boundary reacts with the other rather immobile one, which is pinned by defects, consuming the entire parent hcp phase and leaving a small region of fcc phase, as shown in Figure 1f. The martensitic phase transformation-mediated nucleation process of the  $\{10\bar{1}2\}$  extension twin revealed by our MD

simulations is further schematically illustrated in Figure 1h: the parent hcp phase first transforms to a metastable tetragonal phase, followed by a reverse transformation to a new hcp phase misoriented with respect to the original parent hcp phase, thus forming a twin.

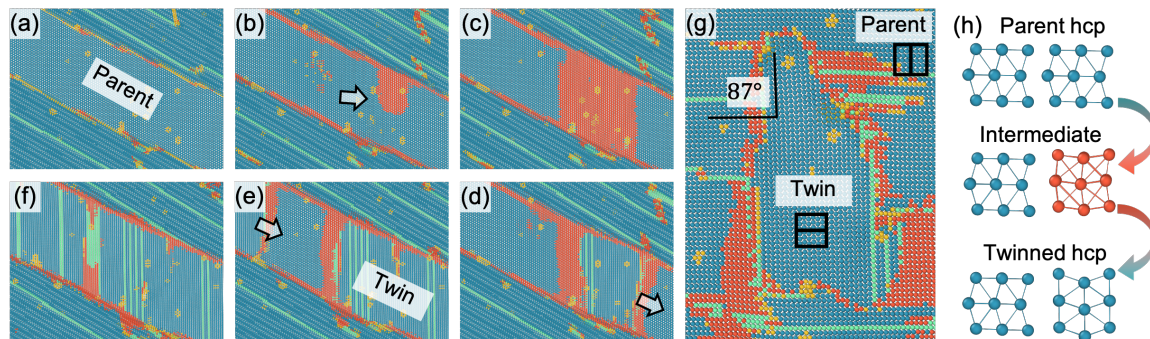


**Figure 1.** Our MD simulation showing the formation of  $\{10\bar{1}2\}$  extension twins through (a,b) hcp-to-tetragonal and (c,d) tetragonal-to-hcp martensitic phase transformations in Mg. The two formed  $\{10\bar{1}2\}$  twin boundaries (e) migrate quickly and (f) react with each other and result in a few layers of fcc phase. (g) A close-up view shows the  $\{10\bar{1}2\}$  twin orientation of the newly formed hcp phase with the parent hcp phase:  $87^\circ$  misorientation across a common  $a$ -axis. (h) Schematic illustration of the twin formation process. Hcp, bcc-like (tetragonal), fcc, and amorphous structured atoms are shown by cyan, red, green, and yellow colors, respectively. In (a–g) the long lines of green atoms are partial stacking faults.

So far, we have demonstrated the complete twinning process observed in our MD simulations, which clearly reveals the critical role of the intermediate metastable tetragonal phase. Notably, this important intermediate state is missing in both the classical “shear-dominated” mechanism [31,32] and the “shuffle-dominated” mechanism [9]. Besides the Wilson potential, the popular Sun potential [33] has been used to verify the same deformation process and similar formation of  $\{10\bar{1}2\}$  twins via the intermediate tetragonal phase is observed. Moreover, the MD simulation has been conducted at 300 K and our martensitic phase transformation-mediated  $\{10\bar{1}2\}$  twin formation process has been reaffirmed. Therefore, our twinning mechanism is applicable over a wide temperature range.

Finally, we emphasize that our twinning mechanism sheds light on the puzzling high formation speed of deformation twins. As early as in 1952, Thompson and Millard reported that  $\{10\bar{1}2\}$  twins can form rapidly in less than  $10^{-4}$  s in hcp cadmium [20]. Such ultrafast twin nucleation speed has led many researchers to seek nucleation mechanisms not requiring the layer by layer gliding of twinning dislocations [1,9,10,15,34]. For example, Cahn concluded that the twin nucleus must be formed as a whole by locally homogeneous shear of the lattice [35]. Given the fact that martensitic phase transformation can occur close to the speed of sound, our twinning mechanism is naturally compatible with the ultrafast twin growth speed, thus, greatly complementing current mechanisms of twin nucleation.

### 3.2. Detailed Structure of the Tetragonal Phase

To further understand the atomic structure of the intermediate phase, we examine ten different regions for many time steps during the twin formation process in our MD simulation and conclude that it is a tetragonal structure. We extract a unit cell (Figure 2a) from our MD simulation and show it in various projections in Figure 2b–d.

There is a less than 2% difference between the two larger lattice parameters of the tetragonal phase during the deformation process. Given that the difference ( $<2\%$ ) is even smaller than the applied strain ( $\sim 3.9\%$ ), this small difference is caused by the applied compressive strain—the lattice is compressed parallel to the loading direction, while the lattice is accordingly elongated perpendicular to the loading direction. We perform further MD simulation to relax the intermediate phase and obtain lattice parameters of  $a = b = 5.27 \text{ \AA}$  and  $c = 3.23 \text{ \AA}$ , confirming that the intermediate phase is tetragonal.

It should be noted that the lattice change from the hcp phase to the tetragonal phase dissipates elastic strain energy, which is the thermodynamic driving force of the twinning process. As shown in the [001] projection (corresponding to the common  $a$ -axis of the  $\{10\bar{1}2\}$  extension twin) in Figure 2b, the tetragonal phase resembles the atomic structure of the  $\{10\bar{1}2\}$  twin boundaries observed in a recent experiment [36] and first-principles calculations [21,37]. Specifically, different from the thin interface structure of a coherent  $\{10\bar{1}2\}$  twin boundary, high-resolution transmission electron microscopy revealed a wide interface structure in an AZ31 alloy [36], in which the atomic structure matches the tetragonal phase observed in our MD simulations during the  $\{10\bar{1}2\}$  twinning process (Figure 2b). In addition, two recent first-principles calculations [21,37] independently predicted the same atomic structure at the saddle point of the energy landscape of the  $\{10\bar{1}2\}$  twinning process in Mg, in which the atomic structures also agree with the tetragonal phase observed in our MD simulations. Below the unit cells in Figure 2b–d, we also show thin slices of our MD simulation during the forward hcp-to-tetragonal phase transformation. It should be noted that the tetragonal phase shows identical atomic structure when projected onto the basal plane (Figure 2c) and the prismatic plane (Figure 2d) of the parent hcp phase.

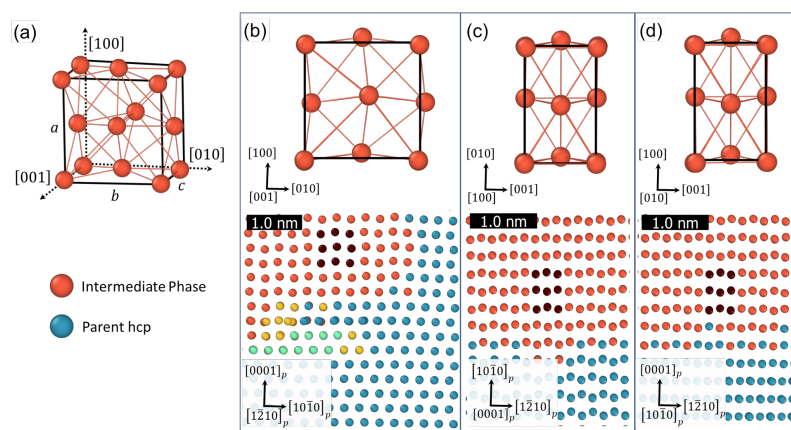


**Figure 2.** (a) A unit cell of the metastable tetragonal phase extracted from our MD simulation. Its different views when projected along (b) [001], (c) [100], and (d) [010] directions. Below each view of the unit cell are thin slices of our MD simulation (b) viewed along the common  $a$ -axis of the  $\{10\bar{1}2\}$  extension twin, (c) projected onto the parent basal plane, and (d) projected onto the parent prismatic plane, in which atoms in one tetragonal unit cell are highlighted in black. The subscript “P” represents the parent hcp phase.

### 3.3. Orientation Relation

The formation of two  $87^\circ$ -misorientated hcp regions through hcp-tetragonal-hcp martensitic phase transformation is not a coincidence, but rather follows a rigorous orientation relation between the crystallographic planes of the parent hcp, intermediate tetragonal, and twin hcp phases. First, by tracing the phase transformations involved in the twinning process, we find that the parent basal plane  $((0001)_{\text{hcp}})$  first transforms into the  $(100)_{\text{T}}$  plane of the tetragonal phase (subscript “T”) and then into the twin prismatic plane  $((10\bar{1}0)_{\text{twin hcp}})$ , while the parent prismatic plane first transforms into the  $(010)_{\text{T}}$  plane and then into the twin basal plane, which is illustrated in Figure 3.

Second, the  $(10\bar{1}2)$  twin plane formed between the parent and twin hcp phases is found to correspond to the  $(1\bar{1}0)_{\text{T}}$  plane of the tetragonal phase. Thus, this lattice correspondence demonstrates that the reversible hcp-tetragonal-hcp martensitic phase transformation follows an orientation relation of:

$$(0001)_{\text{parent hcp}} \parallel (100)_{\text{T}} \quad (1)$$

$$(010)_{\text{T}} \parallel (0001)_{\text{twin hcp}} \quad (2)$$

$$[1\bar{2}10]_{\text{parent hcp}} \parallel [001]_{\text{T}} \parallel [1\bar{2}10]_{\text{twin hcp}} \quad (3)$$

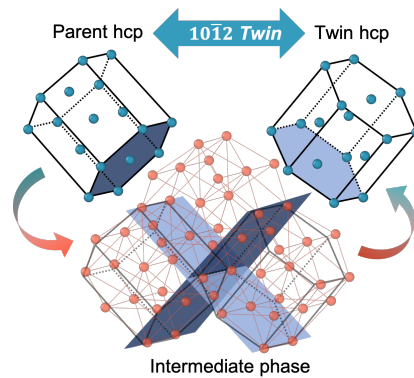


**Figure 3.** Orientation relation of the parent hcp phase, metastable tetragonal phase, and twinned hcp phase. Dark blue represents the parent basal plane and tetragonal (100) plane, and light blue represents the twin basal plane and tetragonal (010) plane. The black lines in the intermediate phase are drawn to show the correspondence between the parent hcp, intermediate, and twin hcp phases.

### 3.4. The Atomic Motion in the Martensitic Phase Transformation-Mediated Twinning Mechanism

Even though our twinning mechanism, involving an intermediate tetragonal phase, is different from the twinning dislocation-based mechanism, herein we will demonstrate that the atomic motions are consistent in the two twinning mechanisms. To achieve this, we trace the two atoms in the motif pair [31] illustrated in Figure 4a and plot their distance perpendicular to the  $\{10\bar{1}2\}$  twin plane during the martensitic phase transformation-mediated twinning process in Figure 4b. The gesture of the motif pair changes gradually during the twinning process: it is up-tilted in the parent hcp phase, flat in the tetragonal phase, and down-tilted in the twin hcp phase. As a consequence, the position of the two atoms flips over, which agrees with the twinning dislocation-based mechanism [38,39] (Figure 4c). Evidently, the twin interface stage in the twinning dislocation-based mechanism (marked in Figure 4c) is essentially the tetragonal phase stage in our mechanism, indicating the agreement between the two twinning mechanisms, yet our mechanism rigorously captures the evanescent intermediate state.

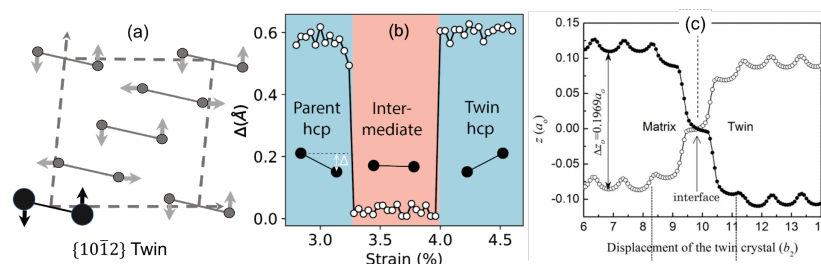


**Figure 4.** (a) The motif pair [31] of atoms traced in our simulation is highlighted, which shuffles perpendicular to the  $\{10\bar{1}2\}$  twin boundary. (b) The evolution of  $\Delta$  during the hcp-tetragonal-hcp martensitic phase transformation, where  $\Delta$  is the distance of the motif pair perpendicular to the  $\{10\bar{1}2\}$  twin plane. The movement of the motif pair in our simulations agrees with (c) the atomic movement in the twinning dislocation-based mechanism [39].  $\Delta$  in (b) corresponds to  $\Delta z$  in (c).

## 4. Conclusions

In summary, we have revealed a rigorous nucleation mechanism of the predominant  $\{10\bar{1}2\}$  extension twin in Mg, which is naturally compatible with the ultrafast twin growth speed. Specifically, the parent hcp phase first transforms to an evanescent metastable tetragonal phase, which subsequently transforms to a twinned hcp phase. Moreover, the atomic motion during the twinning process in our mechanism agrees with that in the twinning dislocation-based mechanism. Our mechanism, emphasizing the evanescent intermediate state of the tetragonal phase, greatly rigorizes the formation process of  $\{10\bar{1}2\}$  twins in hcp metals.

**Author Contributions:** J.O. and A.H.Z. contributed equally to this work. L.C. designed and directed the project. T.M. worked on formal analysis. All authors have read and agreed to the published version of the manuscript.

**Funding:** The authors are partially supported by L.C.'s faculty startup funds from the University of Nevada, Reno. The authors acknowledge the partial financial support from NSF-CMMI Mechanics of Materials and Structures Program (Grant No.#1727428).

**Conflicts of Interest:** The authors declare no conflict of interest.

## References

1. Yoo, M.H. Slip, twinning, and fracture in hexagonal close-packed metals. *Metall. Trans. A* **1981**, *12*, 409–418. [[CrossRef](#)]
2. Sivanandini, M.; Dhami, S.S.; Pabla, B.S. Formability of magnesium alloys. *Int. J. Mod. Eng. Res.* **2012**, *2*, 2464–2471.
3. Barnett, M.R. Twinning and the ductility of magnesium alloys: Part I: “Tension” twins. *Mater. Sci. Eng. A* **2007**, *464*, 1–7. [[CrossRef](#)]
4. Barnett, M.R. Twinning and the ductility of magnesium alloys: Part II: “Contraction” twins. *Mater. Sci. Eng. A* **2007**, *464*, 8–16. [[CrossRef](#)]
5. Christian, J.W.; Mahajan, S. Deformation twinning. *Prog. Mater. Sci.* **1995**, *39*, 1–157. [[CrossRef](#)]
6. Xin, Y.; Wang, M.; Zeng, Z.; Nie, M.; Liu, Q. Strengthening and toughening of magnesium alloy by 10–12 extension twins. *Scr. Mater.* **2012**, *66*, 25–28. [[CrossRef](#)]
7. Xin, R.; Guo, C.; Xu, Z.; Liu, G.; Huang, X.; Liu, Q. Characteristics of long 10–12 twin bands in sheet rolling of a magnesium alloy. *Scr. Mater.* **2014**, *74*, 96–99. [[CrossRef](#)]
8. Mokdad, F.; Chen, D.L.; Li, D.Y. Twin-twin interactions and contraction twin formation in an extruded magnesium alloy subjected to an alteration of compressive direction. *J. Alloys Compd.* **2018**, *737*, 549–560. [[CrossRef](#)]
9. Li, B.; Ma, E. Atomic shuffling dominated mechanism for deformation twinning in magnesium. *Phys. Rev. Lett.* **2009**, *103*, 035503. [[CrossRef](#)]
10. Wang, J.; Yadav, S.K.; Hirth, J.P.; Tomé, C.N.; Beyerlein, I.J. Pure-shuffle nucleation of deformation twins in hexagonal-close-packed metals. *Mater. Res. Lett.* **2013**, *1*, 126–132. [[CrossRef](#)]
11. Chen, P.; Li, B.; Culbertson, D.; Jiang, Y. Contribution of extension twinning to plastic strain at low stress stage deformation of a Mg-3Al-1Zn alloy. *Mater. Sci. Eng. A* **2018**, *709*, 40–45. [[CrossRef](#)]
12. Beyerlein, I.J.; Capolungo, L.; Marshall, P.E.; McCabe, R.J.; Tomé, C.N. Statistical analyses of deformation twinning in magnesium. *Philos. Mag.* **2010**, *90*, 2161–2190. [[CrossRef](#)]
13. Beyerlein, I.J.; Tomé, C.N. A probabilistic twin nucleation model for HCP polycrystalline metals. *Proc. R. Soc. A Math. Phys. Eng. Sci.* **2010**, *466*, 2517–2544. [[CrossRef](#)]
14. Capolungo, L.; Beyerlein, I.J. Nucleation and stability of twins in hcp metals. *Phys. Rev. B* **2008**, *78*, 024117. [[CrossRef](#)]
15. Cayron, C. Hard-sphere displacive model of extension twinning in magnesium. *Mater. Des.* **2017**, *119*, 361–375. [[CrossRef](#)]
16. Koehler, J.S.; Seitz, F.; Read, W.T.; Shockley, W.; Orowan, E. *Dislocations in Metals*; Institute of Metals Division, The American Institute of Mining and Metallurgical Engineers: New York, NY, USA, 1954.
17. Lee, J.K.; Yoo, M.H. Elastic strain energy of deformation twinning in tetragonal crystals. *Metall. Trans. A* **1990**, *21*, 2521–2530. [[CrossRef](#)]
18. Mendelson, S. Dislocation dissociations in hcp metals. *J. Appl. Phys.* **1970**, *41*, 1893–1910. [[CrossRef](#)]
19. Ostapovets, A.; Serra, A. Slip dislocation and twin nucleation mechanisms in hcp metals. *J. Mater. Sci.* **2017**, *52*, 533–540. [[CrossRef](#)]
20. Thompson, N.; Millard, D.J. XXXVIII. Twin formation in cadmium. *Lond. Edinb. Dublin Philos. Mag. J. Sci.* **1952**, *43*, 422–440. [[CrossRef](#)]
21. Zhou, G.; Ye, L.; Wang, H.; Xu, D.; Meng, C.; Yang, R. Energy paths of twin-related lattice reorientation in hexagonal metals via ab initio calculations. *J. Mater. Sci. Technol.* **2018**, *34*, 700–707. [[CrossRef](#)]
22. Zhou, N.; Zhang, G.; Guo, T.F.; Guo, X.; Tang, S.; Huang, X. twin nucleation at prismatic/basal boundary in hexagonal close-packed metals. *Philos. Mag.* **2019**, *99*, 2584–2603. [[CrossRef](#)]

23. Yoo, M.H.; Lee, J.K. Deformation twinning in hcp metals and alloys. *Philos. Mag. A* **1991**, *63*, 987–1000. [[CrossRef](#)]
24. Mendelson, S. Zonal dislocations and twin lamellae in hcp metals. *Mater. Sci. Eng.* **1969**, *4*, 231–242. [[CrossRef](#)]
25. Barrett, C.D.; El Kadiri, H. Impact of deformation faceting on 101-2,101-1 and 101-3 embryonic twin nucleation in hexagonal close-packed metals. *Acta Mater.* **2014**, *70*, 137–161. [[CrossRef](#)]
26. Plimpton, S. *Fast Parallel Algorithms for Short-Range Molecular Dynamics*; Report; Sandia National Labs.: Albuquerque, NM, USA, 1993.
27. Wilson, S.R.; Mendeleev, M.I. A unified relation for the solid-liquid interface free energy of pure FCC, BCC, and HCP metals. *J. Chem. Phys.* **2016**, *144*, 144707. [[CrossRef](#)]
28. Stukowski, A. Visualization and analysis of atomistic simulation data with OVITO—the Open Visualization Tool. *Model. Simul. Mater. Sci. Eng.* **2009**, *18*, 015012. [[CrossRef](#)]
29. Faken, D.; Jónsson, H. Systematic analysis of local atomic structure combined with 3D computer graphics. *Comput. Mater. Sci.* **1994**, *2*, 279–286. [[CrossRef](#)]
30. Honeycutt, J.D.; Andersen, H.C. Molecular dynamics study of melting and freezing of small Lennard-Jones clusters. *J. Phys. Chem.* **1987**, *91*, 4950–4963. [[CrossRef](#)]
31. Crocker, A.G.; Bevis, M. *The Science Technology and Application of Titanium*; Jaffee, R., Promisel, N., Eds.; Pergamon Press: Oxford, UK, 1970; pp. 453–458.
32. Serra, A.; Pond, R.C.; Bacon, D.J. Computer simulation of the structure and mobility of twinning dislocations in HCP Metals. *Acta Metall. Mater.* **1991**, *39*, 1469–1480. [[CrossRef](#)]
33. Sun, D.Y.; Mendeleev, M.I.; Becker, C.A.; Kudin, K.; Haxhimali, T.; Asta, M.; Hoyt, J.J.; Karma, A.; Srolovitz, D.J. Crystal-melt interfacial free energies in hcp metals: A molecular dynamics study of Mg. *Phys. Rev. B* **2006**, *73*, 024116. [[CrossRef](#)]
34. Song, S.; Gray, G., III. Structural interpretation of the nucleation and growth of deformation twins in Zr and Ti—I. Application of the coincidence site lattice (CSL) theory to twinning problems in hcp structures. *Acta Metall. Mater.* **1995**, *43*, 2325–2337. [[CrossRef](#)]
35. Bell, R.L.; Cahn, R.W. The dynamics of twinning and the interrelation of slip and twinning in zinc crystals. *Proc. R. Soc. Lond. Ser. A Math. Phys. Sci.* **1957**, *239*, 494–521.
36. Jiang, S.; Jiang, Z.; Chen, Q. Deformation twinning mechanism in hexagonal-close-packed crystals. *Sci. Rep.* **2019**, *9*, 1–5. [[CrossRef](#)] [[PubMed](#)]
37. Ishii, A.; Li, J.; Ogata, S. Shuffling-controlled versus strain-controlled deformation twinning: The case for HCP Mg twin nucleation. *Int. J. Plast.* **2016**, *82*, 32–43. [[CrossRef](#)]
38. Khater, H.A.; Serra, A.; Pond, R.C. Atomic shearing and shuffling accompanying the motion of twinning disconnections in Zirconium. *Philos. Mag.* **2013**, *93*, 1279–1298. [[CrossRef](#)]
39. Pond, R.C.; Hirth, J.P.; Serra, A.; Bacon, D.J. Atomic displacements accompanying deformation twinning: Shears and shuffles. *Mater. Res. Lett.* **2016**, *4*, 185–190. [[CrossRef](#)]

